Geoinformatics & Geostatistics: An Overview

Research Article

A SCITECHNOL JOURNAL

Assessment of the Sub-Surface Architecture Insights Across the Pan African Belt in Northern Cameroon: Applications of 2.75D Geophysical Modelling of Aeromagnetic Data from the Guider-Kaele Area

Jean Daniel Ngoh[1*], Stephane Assembe[2], Alain Zanga[2], Olivier U. Owono Amougou[1], Paul Claude Ngoumou[3], Kevin L. Mickus[4] and Theophile Ndougsa Mbarga[5]

[1]*Department of Land Surveying, National Advanced School of Public Works, Yaoundé, Cameroon*

[2]*Department of Physics, University of Douala, Douala, Cameroon*

[3]*Department of Geology and Mining Engineering, University of Ngaoundere, Ngaoundere, Cameroon*

[4]*Department of Geography Geology and Planning, Missouri State University, Springfield, USA*

[5]*Department of Physics, University of Yaoundé, Yaoundé, Cameroon*

[*]**Corresponding author:** Jean Daniel Ngoh, Department of Land Surveying, National Advanced School of Public Works, Yaoundé, Cameroon; E-mail: jdngoh@yahoo.fr

Received date: 26 June, 2024, Manuscript No. GIGS-24-139858;

Editor assigned date: 28 June, 2024, PreQC No. GIGS-24-139858 (PQ);

Reviewed date: 12 July, 2024, QC No. GIGS-24-139858;

Revised date: 19 July, 2024, Manuscript No. GIGS-24-139858 (R);

Published date: 26 July, 2024, DOI: 10.4172/2327-4581.1000391.

Abstract

In this study, aeromagnetic data were used to construct a geological model of the Guider-Kaele area in northwestern Cameroon, which is part of the northern segment of the Pan-African belt in Cameroon. The area is dominated by the Poli and Mangbei lithostratigraphic Groups (Neoproterozoic metasedimentary rocks and metavolcanic rocks) intruded by late Pan-African granitoids and tertiary ring complexes. For quantitative analysis, 2.75D forward modelling of these magnetic data was performed using Oasis Montaj v.8.4 along four transects oriented N–S (two lines), NNE–SSW and NNW–SSE. Well log information, borehole data, geologic maps, previous geophysical studies, and Euler deconvolution depth estimates constrained the models derived. In particular, Euler's deconvolution estimated the depth to the magnetic sources (faults and some intrusions) in the 0.39 km to 11.44 km range beneath sea level. Furthermore, the proposed geological models highlight a subsurface composed of a volcanic-sedimentary cover overlying a granitic faulted basement, with some igneous intrusions (doleritic dyke swarms and granodiorites) and several troughs filled with volcanic-sedimentary deposits. In addition, these models reveal that the crust is thinning. The presence of a prominent greenschist layer in this area testifies to the thermal history or degree of metamorphism of its bedrock.

Keywords: 2.75D forward modelling; Pan African belt; Volcano-sedimentary layer; Thermal history; Crustal thinning.

Introduction

Till date, several geological and geophysical studies have been carried out on the Pan-African Belt in Central Africa, with a particular interest in the mapping of crustal formations and their evolution [1,2]. Certainly, the contributions of these works have led to major modifications concerning the Lithostratigraphy and geodynamic evolution of this geological complex. However, despite previous works and the exploitation and mining of marble in the study area, northern Cameroon remains a relatively poorly known and underexplored region. In fact, the Congo Craton-Adamawa-Yade boundary captured almost all the attention of previous works concerning the Pan African belt in Cameroon. Previous studies revealed that this area, because of its pivotal position between the East-Nigeria area in the west, belonging to the Trans-Saharan chain, and the Mayo-Kebbi domain with juvenile crust to the East, and the Adamaoua-Yadé domain, delimited by the Tchollіré-Banyo Fault to the south, would have been intensely affected by successive tectonic events of the Pan-African orogeny [3-7]. As a result, the bedrock characterization in this area is poorly understood and poses problems related to i) the lithostratigraphy; ii) the nature of the contacts (intrusive, sedimentary, tectonic, metamorphic gradient) between the different sets; and iii) tectonic and geodynamic evolution and the implications for mineral resources. The aim of this work is to examine the metamorphic conditions through 2.75D geophysical modelling of aeromagnetic data in the Guider-Kaele area, northern Cameroon.

Geological and tectonic setting

The Guider-Kaele area, which belongs to the Pan African domain in Cameroon, ranges between 09°45' and 10°45'N and 13°15' and 14°30'E. In this area, a soudano-Sahelian climate prevails. The average temperature is between 24°C and 36°C. As a part of the northern domain of the Central African Orogeny Belt (CAOB) in Cameroon, especially the Poli-Lere Group, the study domain consists of medium to high-grade schists and gneisses of volcanic and sedimentary origin that formed in a magmatic back-arc context and Neoproterozoic syntectonic calc-alkaline granitoids [5,7]. The post-Pan African tectonic calc-alkaline granitoids comprise mafic and felsic dykes crosscutting granites and syenite intrusions in schists and gneisses. They align along a NNW-trending line between batholiths [8]. The above units are covered by unmetamorphosed sediments and volcanic rocks in several small basins [7,9]. The Palaeoproterozoic formations and Pan-African batholiths of the Adamawa-Yade domain dominate the far southeast of the study area.

Three tectonic events affected the structural development of this domain, notably a crustal shortening and thickening event caused by collision between Neoproterozoic blocks followed by syn to postorogenic shear movements [7,10]. A crustal shortening event is shown by gentle folding in isoclinal folds with flat-lying foliations formed by thrust faulting [10]. Later, compressional deformation is indicated by vertical and NNE-trending foliations and by tight upright to reclining folds [11]. In the Poli area, this deformation is accompanied by dextral and sinistral shearing (Figure 1) [12].

Aeromagnetic data acquisition and processing

The aeromagnetic data used in this study were acquired from the Africa Magnetic Mapping Project (AMMP) surveys of PGW Ltd. (Paterson, Grant & Watson Limited) in collaboration with GETECH and ITC. The flight path was flown at 235 m above the topographic level with a line spacing of 750 m along the N135°E azimuth. Each individual survey was corrected for diurnal variations and gridded using a standard minimum curvature into one coherent dataset. Then, the regional magnetic field of the Earth or the International Geomagnetic Reference Field (IGRF) was removed from the signal to produce a Residual Magnetic Field (TMI), which was gridded at 1/5 of the flight line spacing and displayed as a colour image. Then, the TMI grid was Reduced to The Equator (RTE) using the inclination and declination angles of the IGRF (-1.01° and -3.96°, respectively). The RTE anomaly map contains both small wavelength anomalies, high-intensity anomalies created by magnetized sources at the surface or at shallow depths, and longer wavelength anomalies related to deeper sources. To amplify the effect of the deeper sources, the RTE data were collected upwards to a height of 1 km above the Earth's surface (Figure 2).

Methodology

The Euler deconvolution method

Euler Deconvolution (ED) is an analytical method based on Euler's homogeneity equation that is used to estimate the apparent locations and depths of several subsurface features, particularly from magnetic or gravitational fields [13,14]. The degree of homogeneity is expressed by the structural index, which measures the fall-off rate of the field with distance from the source, as shown by the following equation from Thompson and Reid et al., (1990):

$$(x-x_0)\frac{\partial T}{\partial x}+(y-y_0)\frac{\partial T}{\partial y}+(z-z_0)\frac{\partial T}{\partial z}=N(B-T)\qquad(1)$$

where:

- (x_0, y_0, z_0): The position of a magnetic source whose total field T is detected at position (x, y, z);
- T: Regional value of the total magnetic field;
- N: The degree of homogeneity, often called the Structural Index (SI), which characterizes the type of source and the rate of variation of the field with distance. The value of N depends on the assumed source geometry.

For magnetic data, N takes values from 0 to 3 [13,14]. Reid et al., showed that only low structural indices (0 to 1) provide the best depth estimates [14]. The Euler depths appear wherever there are lithological discontinuities in the geological formations. They represent the structural and/or stratigraphic changes in various geological formations [15].

Magnetic modelling

For the present study, forward modelling of the source body was performed with the GM-SYS module in Oasis Montaj v8.4 to obtain the optimal fit of the generated source model to the magnetic data. The GM-SYS module helps to calculate the magnetic response from a geological cross-section model.

The methods used to calculate the model's response are based on the methods of Talwani et al., as well as the algorithms described by Won et al., Two-and-a-half-dimensional calculations are based on Rasmussen et al., [16-19]. The GM-SYS inversion routine utilizes a Marquardt inversion algorithm and the USGS computer program SAKI to linearize and invert the calculations [20,21].

Results

Analysis of total magnetic anomaly intensity Reduced to the Equator (RTE)

The RTE magnetic map (Figure 2) reveals anomaly values between -77 and 300 nT, corresponding to magnetic anomalies covering a wide range of amplitudes and wavelengths. A correlation between the anomalies and some morphological features, such as faults, geological contacts and outcrops, can be inferred. Within northwestern Cameroon, these magnetic anomalies seemingly correlate with Proterozoic granitic and metamorphic lithologies, including metavolcanic rocks, gneisses, and schists (Figure 1).

The RTE map contains mainly northeast-trending minima and maxima anomalies that are roughly parallel to the Proterozoic synorogenic strike-slip episodes [10]. The most prominent anomalies are a series of large wavelengths, low-amplitude magnetic maxima (anomalies 1 and 2) and slightly greater magnetic-amplitude minima (anomalies 3 and 4) in the northern portion of the map (Figure 2).

The magnetic maxima are caused by lithologies with lower magnetic susceptibility. Anomalies 1 and 2 occur over the medium to high-grade gneisses of the NW Cameroon terrane and post-Pan African sediments. In contrast, anomalies 3 and 4 occur over metamorphic Precambrian substrata (ectinites and migmatites) overlain by sedimentary formations (Figure 1) [22]. The extent of these low-amplitude magnetic maxima implies that the magnetic susceptibility of the gneisses is relatively low, with some regions (small wavelength maxima within the region of anomaly 1) having higher susceptibility values.

This could be due to high-grade gneisses or isolated mafic or metaigneous bodies [23]. In fact, in the study area, the level of weathering of rocks is highly variable. For example, the outcrops encountered and observed *in situ* show folded, faulted and fractured rocks with some weathering facts available on the ground surface. This weathering impacts the petrographic and geochemical characteristics of rocks and thus the magnetic susceptibility of these rocks.

The upwards continued RTE map exhibits similar patterns of high and low magnetic anomalies, as shown in Figure 2. The upwards continued RTE anomaly ranged from -164.47 to 288.31 nT. The upwards continued RTE map is basically a smoothed version of the RTE map and contains prominent negative (long wavelength) anomalies distributed in the northeastern, central, and southern parts of the study area.

This map clearly highlights positive and negative prominent anomalies roughly elongated in the ENE-WSW direction. The persistence of prominent anomalies with great wavelengths, low-amplitude magnetic maxima (anomalies 1 and 2) and slightly greater-amplitude magnetic minima (anomalies 3 and 4) observed in the northern portion of the map (Figure 3) shows that they are associated with deeper structures. In addition, the upwards continued RTE map shows attenuated anomalies (anomalies 8, 9 and 10) that are also related to upper crustal lithologies (Figure 3).

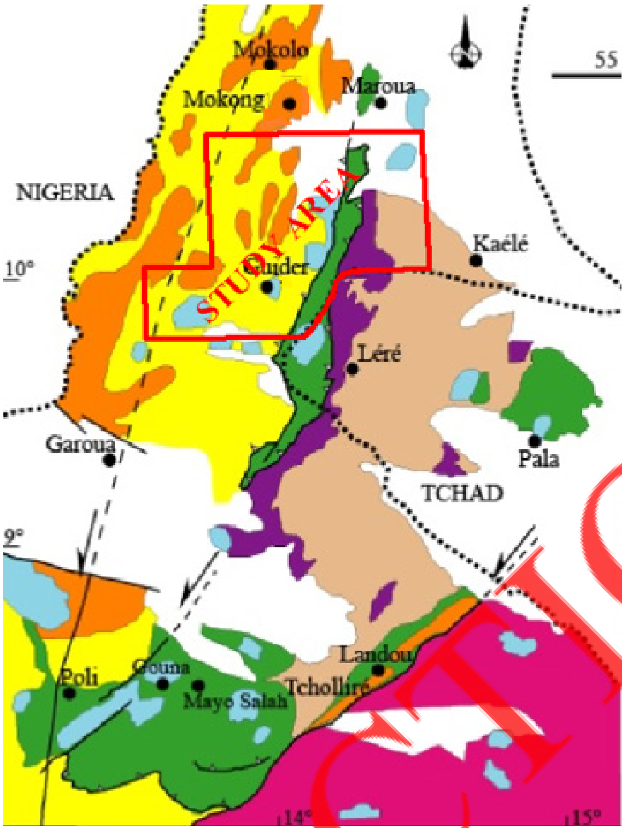

Figure 1: Simplified geologic map of the study area (Penaye et al., 2006, modified as a document available in a public domain). **Note:** 1-Post-Pan-African sediments (⌐); 2-Late to posttectonic Pan-African granitoids (■); 3-Syntectonic granites (■); 4-Mayo-Kebbi batholith: tonalites, trondhjemites and granodiorites (■); 5-Medium-to high-grade gneisses of the NW-Cameroon domain (■); 6-Mafic to intermediate complex of the Mayo-Kebbi domain (metadiorites and gabbro diorites) and amphibolites (■); 7-Neoproterozoic low-to medium-grade volcano-sedimentary sequences of the Poli-Léré Group (■); 8-Remobilized palaeoproterozoic Adamawa-Yadé domain (■); 9-Thrust front (⊤); 10-Strike-slip fault: Tcholliré-Banyo shear zone, Godé-Gormaya shear zone, Balche shear zone (⁄); 11-State border (⁄).

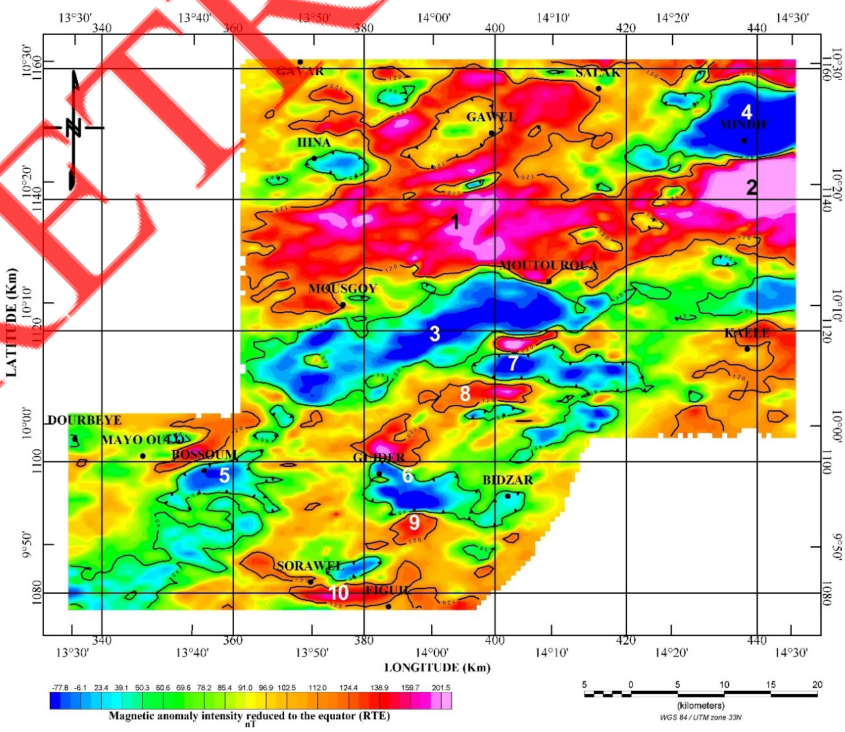

Figure 2: Total magnetic anomaly intensity reduction to the equator map of the study area.

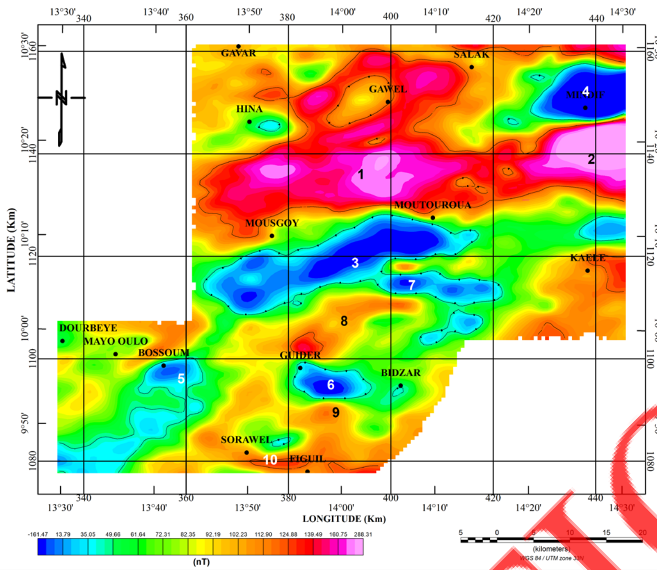

Figure 3: RTE map upwards continued to 1 km above the Earth's surface.

The distribution of these different patterns clearly suggests that the study area is characterized by zones of high and low magnetic susceptibility within different lithologies at depth. Microfaults and microfolds observed in the field were more developed and prevalent within some metamorphic rocks. The structures have various strikes (NE-SW, NNE-SSW and E-W) and subvertical dips, in accordance with the regional structures controlling them. These faults could have been caused by vertical movements due to subsidence of the basin and lateral movements due to shearing and could have affected the substratum [24]. Mapping observations revealed that there was more than one deformation phase. The geodynamic environment corresponds to a sedimentary basin (Mayo Oulo-Lere basin) put in place during the initiation of the South Atlantic opening [22].

Depth estimates

The Euler deconvolution technique is an analytical method chosen for detecting the locations and depths of different features from obtained anomalies. This study focuses on geological boundaries, faults and dyke locations. The structural indices used are 0.25 and 1.25, corresponding to ideal geometrical contacts and faults, respectively [25]. Euler deconvolution is applied to the magnetic RTE field with a 20 km × 20 km window size in the Oasis Montaj Program v.8.4, which provides better resolution for the solutions. The obtained Euler's solution maps are shown in Figures 4a and 4b. These solutions are relatively consistent with short and long-wavelength anomalies related to different tectonic features and some lithological formations in the study area. The depths of the faults and contacts ranged from 0.39 km to 11.44 km in the NNW-SSE, NE-SW, NW-SE, and E-W directions.

Euler solutions for structural index SI=0.25: The solutions for a structural index of 0.25 (Figure 4a) are located between 0.39 km and 6.6 km depth, with an average depth of 2.32 km. These solutions are more clustered and mainly follow the NW-SE, NE-SW and E-W directions. Most of these solutions represent deep-seated structural features. The surface features and resulting lineaments are located above 0.39 km in depth. The moderately deep-seated solutions are in the central, eastern and southwestern parts of the study area, while the depth solutions of other parts of the area are relatively shallow under an average depth, thus inferring shallow magnetic anomaly sources. In accordance with the geodynamic model proposed by Toteu et al., the configuration observed in the area suggests the presence of two collisional blocks: The southern block with a passive and older margin and the northern block with an active margin [7]. This collision generated intense deformation in the North Cameroon domain due to the penetration of the rigid block into the active margin (Figure 4a) [26].

Euler solutions for structural index SI=1.25: The Euler solutions for the structural index of 1.25 (Figure 4b) provide a depth range from 0.76 km to 11.44 km. As shown previously, there are more similarities and clusters of solutions with solutions for a structural index of 0.25. The observed abundance of solutions in the study area implies the existence of a broad set of dykes or vertical faults. These clusters are crosscut by those due to deep magnetic sources (≥ 5 km) oriented NE-SW, which have linear stacks of solutions predominant in the NE-SW, NNW-SSE, E-W and NW-SE directions. There is a lack of solutions in the northern, western, eastern, and southern margins of the study area (Figure 4b).

The patterns of Euler depths obtained by interpolation of each structural index are similar and show that the bedrock of the study area is strongly affected by intermediate and deep tectonic features (≥ 3 km), which seem not to exceed a depth of 7 km. The values obtained are within the range of those obtained by previous researchers in the area. There is also a concentration of deep magnetic sources mainly along the NE-SW to ENE-WSW directions. This zone is particularly a large-scale apparent average depth zone oriented along the Mousgoy-Moutourouа axis, which would have imposed these preferential directions in both cases. This axis, which contains a set of granitoids and orthogneisses, would therefore be dominated by the structural imprint of the metagongroses of the Mayo-Kebbi domain. Some previously known lineaments and features in the area are highlighted through a clustering of solutions that coincide with their directions. Then, a general trend in the zone of weakness can be observed and linked to the regional tectonic features encountered in the study area.

According to both Euler maps, the northeastern area has no more solutions, which implies extremely weak tectonics in that zone. The deepest geological features are located below 5 km; they follow the NNE-SSW, E-W and NNW-SSE directions and dominate the study area (Figures 5a and 5b).

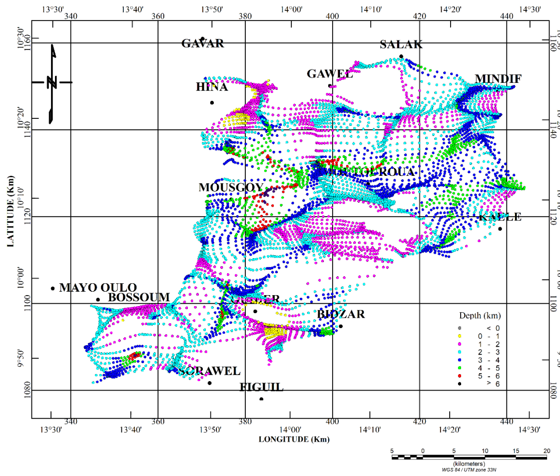

Figure 4a: Euler solutions for SI=0.25.

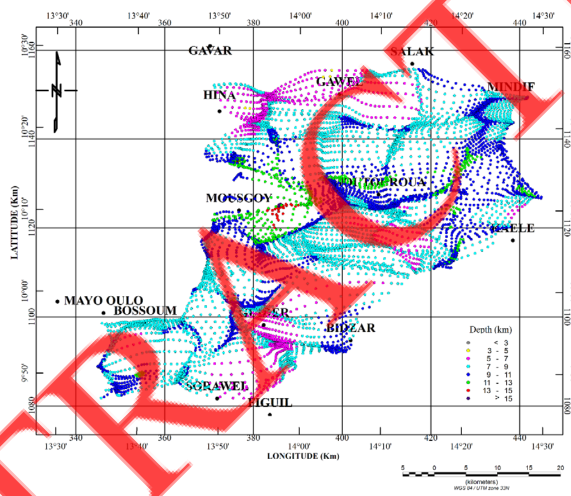

Figure 4b: Euler solutions for SI=1.25.

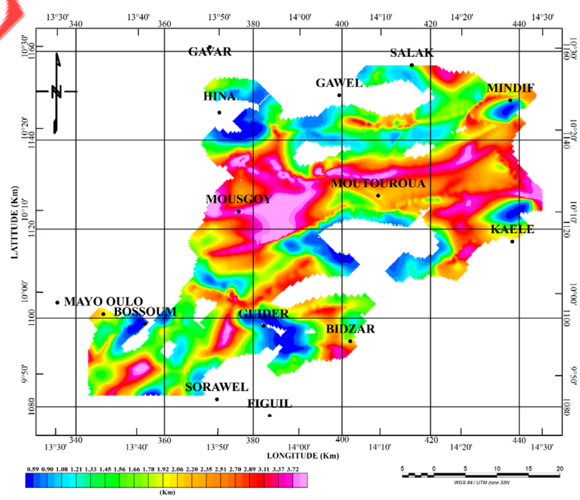

Figure 5a: Euler depth map of the study area for SI=0.25.

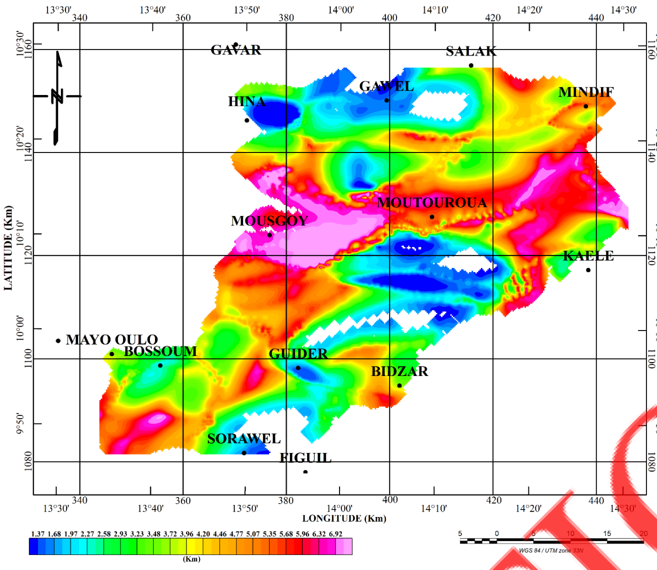

Figure 5b: Euler depth map of the study area for SI=1.25.

Magnetic modelling

In general, the shape of an anomaly can help to determine the shape and position of density or magnetic contrasts. Theoretically, several geometries will fit a particular anomaly. However, in practice, using realistic geological or other geophysical controls, anomaly fits provide real numerical constraints on anomaly sources [27]. Furthermore, the shape and amplitude of the magnetic response depend on many other variables in addition to the concentration of magnetic minerals present, which include the geometry and depth of the deposit, its orientation relative to the magnetic field to the north and the inclination of the Earth's magnetic field at its location [27,28].

In this study, four geological cross sections were modelled from the RTE map with a 2.75D forward modelling approach in GM-SYS. These models were constrained by geological knowledge, borehole data with a maximum depth of 69 m and Euler depths of the study area, and models with a Root Mean Square (RMS) less than 5% were accepted (Figure 6) [24].

Profile 1: The magnetic north–south cross-section P1 is situated near the Mindif-Kaele axis and is approximately 56 km long. Along this transect, the magnetic field anomaly intensity oscillates between -255.42 nT and 363 nT (Figure 7). This is possibly caused by subsurface discontinuities or major formations. The magnetic field decreases to -255.42 nT at approximately 11.4 km, while it peaks at 363 nT at approximately 19.3 km from the north. This variability in the magnetic field intensity along the transect reflects the heterogeneity of the Earth's crust (Figure 7).

The modelled geological section highlights a subsurface sequence formed by a sedimentary cover including detrital sediments, lagoon-lacustrine sandstones, or arkose-sandstones with a magnetic susceptibility of 0.0209 SI. The latter are bottomed by schists (with a magnetic susceptibility of 0.003 SI), which overlie a crystalline, tabular, and faulted basement.

The whole basement consists of gneissic and granitic formations (syn-tectonic granites) with susceptibilities of 0.025 SI and 0.05 SI, respectively. This geological model also highlights a prominent intrusion or batholith overlain by sedimentary formations that extend down beyond 10 km depth into the crystalline basement. The magnetic susceptibility (0.051 SI) of this intrusive batholith suggested that it could be a granodiorite or syenogranite, which are members of the granitoid group. In addition to the observed batholith, this model also reveals a strongly faulted crystalline basement that allowed small magmatic intrusions or magmatic lift during metamorphism.

The progressive uplift of the crystalline basement formations from north to south suggests a zone of surrection, the consequence of which would be the rise of the granito-gneissic or granito-migmatitic basement, which would result from the Pan-African orogeny. In addition, given the stratigraphy and apparent geometry of the basement, this geological model reveals a sedimentary basin with crystalline bedrock, which, according, constitutes the envelope form and emphasizes the synclinal termination of the Maroua volcano-detrital vein [29].

Profile 2: Magnetic profile P2 is also north-south, measures approximately 84 km in length, and cuts the study area longitudinally along the Guider-Figuil axis. Along this transect, the observed magnetic field anomaly varies from -67.9 to 210 nT. The profile is irregular, and the occurrence of many peaks indicates the presence of discontinuities or geological features (Figure 8). The fairly high magnetic signal in contrast to that in the first profile is a probable signature of near-surface high magnetic susceptibility formations.

Like in transect P1, the geological model is a three-layered subsurface. The sedimentary cover (k=0.0209 SI) consists of limestone, conglomeratic arkosic and ferruginous sandstone layers; then, a schist layer (k=0.003 SI) is bottomed by a basement made up of gneisses (k=0.025 SI) and granites (k=0.05 SI) (Figure 8).

In addition, this geological model highlights intense fracturing of the crystalline substratum, whose northern block seems to have collapsed while the southern block has moved up. This apparent configuration suggests the existence of multiple faults with vertical displacement and justifies the presence of a crystalline basement uplift observed along this cross section. Therefore, the model's general architecture suggests that regional metamorphism heavily affected the local basement. This general architecture and the lithology derived from the model therefore highlight that the combined effects of intense tectonic activity and regional metamorphism heavily affected the basement of this area.

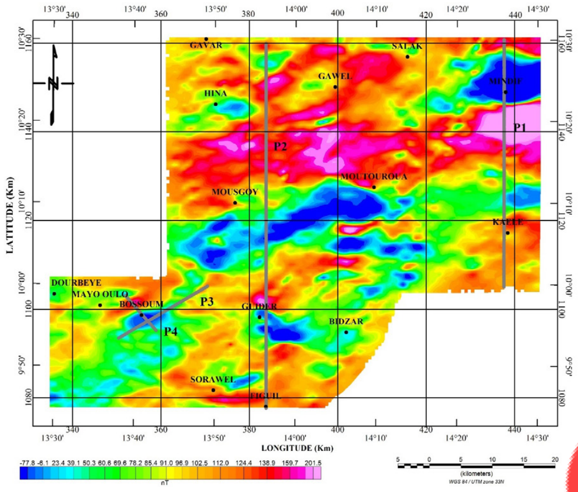

Figure 6: Total magnetic anomaly intensity reduction to the equator map of the study area with the locations of different profiles.

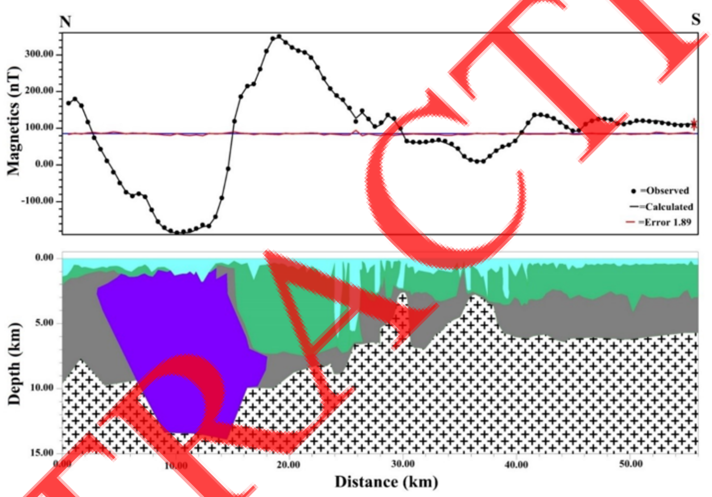

Figure 7: Model of profile 1. **Note:** Granitic basement (0.05 SI) (); Schist (0.003 SI) (); Gneiss (0.025 SI) (); Sandstone conglomerate (0.0209 SI) (); Magnetic intermediate intrusions ().

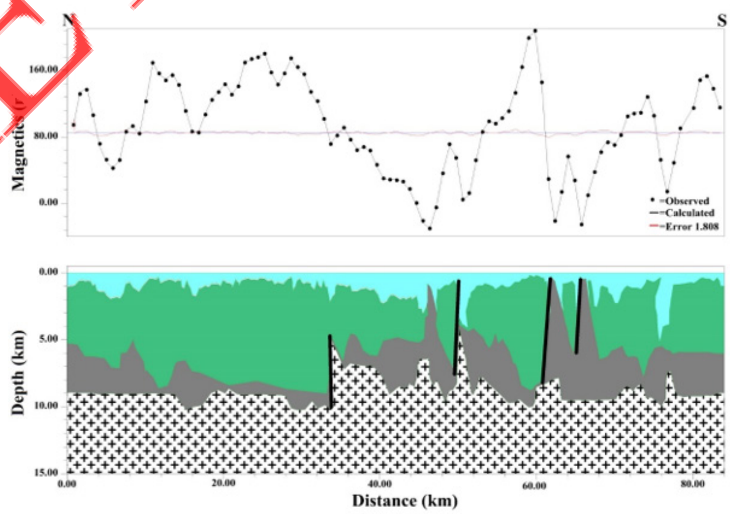

Figure 8: Model of profile 2. **Note:** Granitic basement (0.05 SI) ();Schist (0.003 SI) (); Gneiss (0.025 SI) (); Sandstone conglomerate (0.0209 SI) (); Fault ().

Profile 3: The magnetic cross-section P3 is approximately 33 km in length in the NE–SW direction and is located in the Bossoum-Dourbeye surroundings. Along this transect, the intensity of the magnetic field anomaly oscillates between -55 and 155 nT. The 2.75D modelled subsurface sequence shows a downwards sedimentary cover lying on top of the schists, and these two geological formations (sedimentary cover and schists) overlie a crystalline faulted basement, which consists of gneisses and granites. The model also highlights a dolerite (k=0.062 SI) rooted in the gneisses, which would have been emplaced during the syn-orogenic reactivation phases. Therefore, this hypabyssal intrusion resulted from swarms of dikes emanating from a large intrusive body at depth and was facilitated by fracturing of the gneissic formations or lithostratigraphic contact (Figure 9).

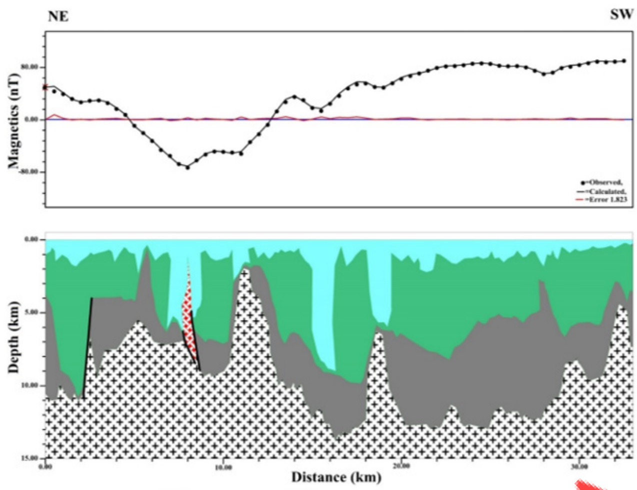

Figure 9: Model of profile 3. **Note:** Granitic basement (0.05 SI) (⁂);Schist (0.003 SI) (■); Gneiss (0.025 SI) (■); Sandstone conglomerate (0.0209 SI) (■); Doleritic intrusions (0.062) (■); Fault (⁄).

Profile 4: Magnetic profile P4 extends more than approximately 10.40 km in the NW–SE direction and intersects profile P3. Herein, the magnetic field intensity ranges between -60 nT and 160 nT, with only two peaks, which could be due to the presence of an important geological structure or formation.

The geological model almost conforms with the previous models despite some differences in the shape and amplitude of the anomaly. From northwest to southeast, there is a relative rise (thickening) of the granitic bedrock and thus a thinning of the sedimentary cover, probably resulting from regional isostatic compensation. Like the previous model, this model also suggests the presence of a synform or syncline with a granitic-gneissic basement filled by schist formations.

Fracturing with granitic basement infiltration occurs near the northern flank. The southern flank of this syncline was subjected to major fracturing of the granitic bedrock, which was filled by the schist layer. These subsurface faults, fractures, or parts of the geological layers could test the extent and impacts of the tectonic events that occurred during the Pan African orogeny (Figure 10).

In addition, the modelled crystalline basement sometimes collapsed or rose and was dotted with subbasins of the sedimentary layer. From northwest to southeast, the geomorphology of this granitic basement suggests an uplifted zone, which results from isostatic compensation, and the presence of a probable granitic unconformity or schistogneissic layer affected by an extensional trough. The thickness of the schist layer, which results from the metamorphism of sedimentary formations with carbon or clayey materials, indicates the extent of the sinking of this synform or syncline.

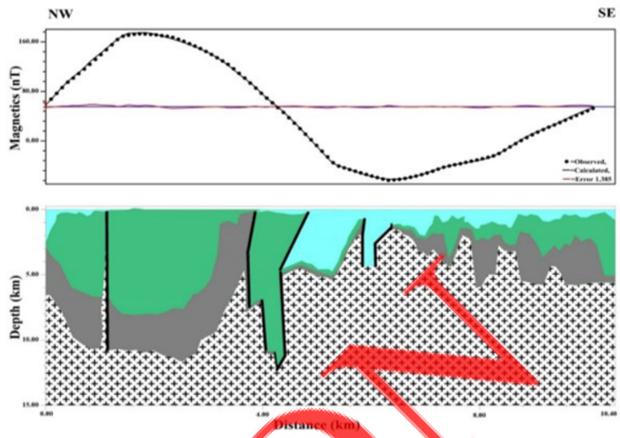

Figure 10: Model of profile 4. **Note:** Granitic basement (0.05 SI) (⁂);Schist (0.003 SI) (■); Gneiss (0.025 SI) (■); Sandstone conglomerate(0.0209 SI) (■); Fault (⁄).

Discussion

The Euler deconvolution solution map highlights more clustered solutions from south to north of the study area. Generally, the Euler solutions for different structural indices show a depth range of 0.39 km to 11.44 km (Figure 4a and 4b). The greatest depth of geological features is found in the central part of the study area and is relatively scattered around the southwestern edge. The basement rocks in the northwest and southeast regions are relatively shallow. These clustered solutions highlighted several main E-W, NE-SW and NW-SE trends, which fit the regional trends. With regard to the major directions, spatial distributions, and roof depths of the investigated structures obtained by the application of Euler's deconvolution method, these geological formations would indeed be deep-seated. The structural trends highlighted suggest that the main NE geological feature is the tectonic imprint of the Katanguian orogeny, which controls the tectonic arrangement of the Pan-African domain and was confirmed by the Massenya-Ounianga heavy gravity anomaly line [2,30]. In addition, according to some authors, this dominant structural trend could also be due to the opening of the South Atlantic Ocean, for which the direct insight was the collapse of the unstable corridor of northern Cameroon and southern Chad, with a main NNE–SSW structural trend. Thus, this configuration suggests the earlier hypothesis for global NE–SW geological and tectonic features [30-33].

The geological models obtained through 2.75D modelling highlight a mainly faulted geological environment. These geological models revealed sedimentary, metamorphic, and igneous formations overlying a syntectonic granitic basement. The presence of strongly foliated metamorphic rocks such as schists and gneisses in this area suggests that this region could either have been affected by regional metamorphism or originated from deformation under differential stress conditions resulting from tectonic forces, as witnessed by the several metamorphosed rocks occurring in the eroded mountain chain (e.g., as seen in Mindif surroundings) [34]. The hypothesis of regional metamorphism seems to be confirmed by the presence of a thick schist layer in the four subsurface 2.75D models. In addition, according to previous geophysical works and geological information, with regard to the geometry, thickness, and spatial disposition of layers, the dominant metamorphic facies in the area under study result from high-temperature and high-pressure geothermal gradients [1,30,35,36].

These geological models also highlighted faulting and a southwards progressive thickening of the crust. This occurs because the crust in that area sinks farther either to compensate for the added weight or to react to compressional stresses in the rocks due to tectonic forces. The upwelling or crustal thinning zones, considering the hypothesis of an isostatic phenomenon, could be due to a shallow or deep prominent magmatic source. Several authors have linked this configuration to the tectonic accidents affecting this region [1,36]. For example, those affecting Central Cameroon with the establishment of horsts represented by the Adamawa granites or an E-W extension phase prevailed on the Cameroon Volcanic Line [37,38]. Therefore, the several probable subbasins observed in these modelled transects could result from the manifestations of regional isostatic compensation following the elevation of the Adamawa horst, which is in isostatic equilibrium at altitudes below 1000 m [35]. In addition, since the Pan-African belt, in which the study area is located, underwent various tectonic events marked by several rifting phases characterized by prerift deformation followed by crustal thinning. Accordingly, with the idea of crustal thinning on a regional scale seems more plausible [30].

Furthermore, the modelled sections revealed several high magnetic signatures interpreted as intrusions with different susceptibility values. These intrusions vary from one profile to another and suggest potential mineralization zones in this region. Their presence could result from the upwelling of igneous material in the area, probably through diapiric activity, which is a sliding regime leading to the segregation of granodioritic magma [39]. In fact, the green schist facies encountered in the field results from thermal changes leading to the transformation of clays (shale) and limestone into schists and marble, respectively, reaching the green schist facies. This modified the original stratification of the layers observed in the field, giving them a subvertical dip. This hypothesis could explain the presence of high magnetic susceptibility (k=0.051 SI) granodiorites observed in profile P1 near Mindiff and another high susceptibility intrusion (k=0.062 SI) in profile P3. In addition to syntectonic plutonism resulting in occasional erosion of orthogneisses, this area records Pan-African late and postorogenic intrusive rocks such as Mindiff syenite or granodioritic rocks. The evidence of these various intrusive bodies is facilitated by a densely fractured basement, which allows upwelling of mantle materials leading to several batholiths or dikes, swarms all emanating from a large intrusive body at depth. These faults likely weaken the crust in various areas; if they are not filled by crustal material, they are filled by sedimentary or volcano-sedimentary formations.

Conclusion

In this region, magnetic modelling of the four profiles improved on the reduced-to-equator anomaly map. The Reduced to Equator anomalies (RTE) map displays magnetic anomalies covering a wide range of amplitudes and wavelengths, with a relatively good correlation between the anomalies and some morphological features, as observed in northwestern Cameroon. The reduced to equator anomalies map presents mainly northeast-trending minima and maxima anomalies that are roughly parallel to the strike-slip tectonic episodes. Euler's deconvolution highlights more clustered solutions from south to north characterized by depth values ranging from 0.39 km to 11.44 km. These clustered solutions highlighted several main E-W, NE-SW and NW-SE trends, which fit the regional trends. The 2.75D forward models obtained highlight faulted and folded geological facies characterized by the presence of several metamorphic rocks. This study suggested that the area was affected by many tectonic features during the Pan African orogeny. Several unconformities materialized by folded and faulted basement or synclinal troughs separated by anticlinal ridges have been highlighted.

References

1. Nguimbous-Kouoh JJ, Ndougsa-Mbarga T, Njandjock-Nouck P (2010) The structure of the Goulfey-Tourba sedimentary basin (Chad-Cameroon): A gravity study. Geofis Int 49(4):181-193.
2. Abate Essi JM, Marcel J, Yene Atangana JQ, Ahmad AD, Fita Dassou E, et al. (2017) Interpretation of gravity data derived from the Earth Gravitational Model EGM2008 in the Center-North Cameroon: Structural and mining implications. Arab J Geosci 10:1-3.
3. Ferré EC, Caby R, Peucat JJ, Capdevila R, Monié P (1998) Pan-African, post-collisional, ferro-potassic granite and quartz-monzonite plutons of Eastern Nigeria. Lithos 45(4):255-279.
4. Ferré E, Gleizes G, Caby R (2002) Obliquely convergent tectonics and granite emplacement in the Trans-Saharan belt of Eastern Nigeria: A synthesis. Precambrian Res 114(4):199-219.
5. Penaye J, Kröner A, Toteu SF, Van Schmus WR, Doumnang JC (2006) Evolution of the Mayo Kebbi region as revealed by zircon dating: An early (ca. 740 Ma) Pan-African magmatic arc in southwestern Chad. J Afr Earth sci 44(5):530-542.
6. Isseini M (2011) Neoproterozoic crustal growth and differentiation: Example of the Mayo Kebbi massif in southwestern Chad
7. Toteu SF, Penaye J, Djomani YP (2004) Geodynamic evolution of the Pan-African belt in central Africa with special reference to Cameroon. "Can J Earth Sci 41(1):73-85.
8. Toteu SF, Penaye J, Deloule E, Van Schmus WR, Tchameni R (2006) Diachronous evolution of volcano-sedimentary basins north of the Congo craton: Insights from U–Pb ion microprobe dating of zircons from the Poli, Lom and Yaoundé Groups (Cameroon). J Afr Earth Sci 44(45):428-442.
9. Van Schmus WR, Oliveira EP, Da Silva Filho AF, Toteu SF, Penaye J, et al. (2008) Proterozoic links between the Borborema province, NE Brazil, and the central African fold belt. Geol Soc Spec Publ 294(1):69-99.
10. Ngako V, Affaton P, Njonfang E (2008) Pan-African tectonics in northwestern Cameroon: Implication for the history of western Gondwana. Gond Res 14(3):509-522.
11. Ngako V, Njonfang E (2011) Plates amalgamation and plate destruction, the western Gondwana history. in: D. closson (Ed.), tectonics. INTECH 3-34.
12. Dawaï D, Bouchez JL, Paquette JL, Tchameni R (2013) The Pan-African quartz-syenite of Guider (north-Cameroon): Magnetic fabric and U–Pb dating of a late-orogenic emplacement. Pre Res 236:132-144.
13. Thompson D (1982) EULDPH: A new technique for making computer-assisted depth estimates from magnetic data. Geophys 47 (1):31-37.
14. Reid AB, Allsop JM, Granser H, Millett AT, Somerton IW (1990) Magnetic interpretation in three dimensions using Euler deconvolution. Geophys 55(1):80-91.
15. Clotilde OA, Tabod TC, Séverin N, Victor KJ, Pierre TK (2013) Delineation of lineaments in South Cameroon (Central Africa) using gravity data. O J Geology. 2013.
16. Talwani M, Worzel JL, Landisman M (1959) Rapid gravity computations for two-dimensional bodies with application to the Mendocino submarine fracture zone. J Geophy Res. 64(1):49-59.
17. Talwani M (1964) Computation of magnetic anomalies caused by two dimensional structures of arbitary shape. Com Min Indust.1:464-80.
18. Won IJ, Bevis M (1987) Computing the gravitational and magnetic anomalies due to a polygon: Algorithms and Fortran subroutines. Geophysics. 52(2):232-8.
19. Rasmussen R, Pedersen LB (1979) End corrections in potential field modeling. Geophy Prosp. 27(4):749-60.
20. Marquardt DW (1963) An algorithm for least-squares estimation of nonlinear parameters. Journal of Indust App Mathematics;11(2):431-41.
21. Webring M (1985). Semi-automatic Marquardt inversion of gravity and magnetic profiles. US Geo Sur File Report. 1985:85-122.
22. Regnoult JM. Geological summary of Cameroon. 1986.

23. Ngoh JD, Mbarga TN, Mickus K, Tarek Y, Tabod TC (2020) Estimation of Curie Point Depth (CPD) across the pan African belt in Northern Cameroon from aeromagnetic data. O J Earthquake Res. 9(3):217-239.

24. Cimencam SA (2016) Final exploration report and Resource estimation: A NI 43-101 Technical Report on Marble Resource.

25. Barbosa VC, Silva JB, Medeiros WE (1999) Stability analysis and improvement of structural index estimation in Euler deconvolution. Geophysics. 64(1):48-60.

26. Abdelsalam MG, Liégeois JP, Stern RJ (2002) The saharan metacraton. J African Earth Sci.34(3-4):119-36.

27. Prieto C, Pratsch J (2000) Gulf of Mexico study links deep basement structures to oil fields. Offshore. 60(6):116-7.

28. Obi D (2011) Specific issues on gravimetric and magnetic methods of geophysical exploration. European Sci Res. 48(3):399-423.

29. Bessoles B, Trompette R (1980) Geology of Africa, the Pan-African chain" mobile zone of central Africa (southern part) and Sudanese mobile zone. 92: 396.

30. Djomani YP, Nnange JM, Diament M, Ebinger CJ, Fairhead JD. (1995) Effective elastic thickness and crustal thickness variations in west central Africa inferred from gravity data. J Geo Res Solid Earth.100(B11):22047-70.

31. Loule JP, Lumbomil P (2009). The Logone Birni Basin (LBB) in Northern Cameroon: Transition between the West African Rift Sub-System (WAS) and the Central African Rift Sub-System (CAS); Tectonic and Geophysical Models.

32. Sylvestre G, Paul NJ, Timoléon N, Boniface K, Djibril KN (2010) Polyphase deformation and evidence for transpressive tectonics in the Kimbi area, Northwestern Cameroon Pan-African fold belt. J Geo Mining Res. 2(1):001-15.

33. Cornacchia MA, Dars RE (1983) A major structural feature of the African continent; the Central African lines from Cameroon to the Gulf of Aden. Bulletin Soc Géolog France.7(1):101-9.

34. Stephen AN (2018) Petrology.

35. Poudjom DY(1993) Contribution of gravimetry to the study of the continental lithosphere and geodynamic implications: Study of an intraplate bulge: The Adamawa massif (Cameroon). Th Géophys Université Paris. 11: 295.

36. Kamguia J, Manguelle DE, Tabod CT, Tadjou JM (2005) Geological models deduced from gravity data in the Garoua basin, Cameroon. J Geophy Eng. 2(2):147-52.

37. Popoff M (1983) Geodynamic approach to the Benoue trench (NE Nigeria) based on field data and remote sensing. Bull Cen Rech Expl Prod Elf Aq.7:323-37.

38. Reusch AM, Nyblade AA, Wiens DA, Shore PJ, Ateba B, et al. (2010) Upper mantle structure beneath Cameroon from body wave tomography and the origin of the Cameroon Volcanic Line. Geochem Geophy Geosys.11(10).

39. Pons J, Barbey P, Dupuis D, Léger JM (1995) Mechanisms of pluton emplacement and structural evolution of a 2.1 Ga juvenile continental crust: The Birimian of southwestern Niger. Precam Res. 70(3-4):281-301.